Stabilization of Collective Motion in a Time-Invariant Flowfield on a Rotating Sphere

Sonia Hernandez and Derek A. Paley

Abstract— We provide Lyapunov-based control laws that stabilize relative equilibria in a model consisting of particles that travel on the surface of a rotating sphere in a time-invariant flowfield. These control laws are of interest because they have applications in planetary-scale mobile sensing networks in air and sea. A rotating sphere is introduced so that the particles are subject to the Coriolis effect that occurs on the Earth. A point vortex generates a time-invariant flowfield in the model and depicts naturally occurring phenomena such as ocean currents, hurricanes, and tornadoes. We show that particles can be steered into circular formations in a time-invariant flow using a theoretically justified algorithm. Simulations show that the same algorithm stabilizes circular formations in a time-varying flow, and this draws particular interest because it suggests that formations of autonomous vehicles could potentially be used in real–world applications.

I. Introduction

Stabilization of collective motion of multiple autonomous vehicles using feedback control laws provides a robust sensing methodology for synoptic and adaptive sampling in air [1] and sea [8]. For example, autonomous underwater gliders provide a robust platform for synoptic data collection of spatiotemporal processes in the ocean [2]. It is difficult to coordinate the motion of autonomous vehicles due to external flowfields such as ocean currents, atmospheric winds and hurricanes. This challenge highlights the need to develop theoretically justified algorithms that stabilize collective motion in the presence of a flowfield [3], [12].

Previous work on collective motion in a flowfield has focused on a planar model of self-propelled particles [6], [7], [10]. A planar model is sufficient for stabilizing collective motion in a small-scale operating domain. However, motivated by unmanned vehicles that operate in large planetary-scale sensing networks—such as underwater gliders and long-endurance aircraft—we are interested in studying a spherical model in the presence of an external flow. Most of the work done in non-planar collective motion has been focused on limited communication and flow-free models [5], [13], [11]. We extend this work by studying collective motion in a time-invariant flowfield on a rotating sphere.

This paper extends [11], which describes a system of self-propelled particles traveling on the surface of a non-rotating sphere in a flow-free model. It parallels the development in [12], which describes a planar frame work for collective

S. Hernandez is a graduate student in the Department of Aerospace Engineering, University of Maryland, College Park, MD 20742, USA `hernans@umd.edu`

D. A. Paley is an Assistant Professor in the Department of Aerospace Engineering, University of Maryland, College Park, MD 20742, USA `dpaley@umd.edu`

motion in a time-invariant flow. We study the case of a rotating sphere because we are interested in creating a model that incorporates the Coriolis effect. We also study the specific case of a point vortex acting as a time-invariant flowfield because this creates an Earth-like environment in which the point vortex represents a naturally occurring phenomenon, such as an ocean current, hurricane, or tornado.

We provide Lyapunov-based control algorithms to stabilize circular formations on the rotating sphere in a time-invariant flow. We give an example of stabilization of collective motion in the presence of a single point vortex that generates a time-invariant flowfield. We also show that, in the presence of two point vortices whose relative motion generates a time-varying flowfield, circular formations of particles are still generated.

The paper is organized as follows. In Section II we describe a model of self-propelled particles that move at constant speed on the surface of a rotating sphere. This framework includes a time-invariant flowfield. In Section III we provide control algorithms to stabilize circular formations on a rotating sphere in a time-invariant flow. In Section IV, we present an example in which the flowfield is generated by point vortices on the sphere. Section V summarizes our results and discusses future work.

II. Particle/Flow Model on a Rotating Sphere

The model studied in the present paper extends the model introduced in [11], which consists of N identical particles moving at a constant speed on the surface of a sphere. We expand this framework by introducing rotation to the sphere and adding a time-invariant flowfield to the model. Since we are dealing with particles, we assume that they cannot collide.

A. Self-Propelled Particle Dynamics

The particle dynamics of the flow-free and non-rotating system were derived in [11] and are summarized here. The model consists of N particles moving at a constant speed $\rho_0 s_0$ on the surface of a sphere with radius ρ_0 and center O. The position of particle k, where $k \in \{1, \ldots, N\}$, relative to O is represented by $\mathbf{r}_k$ (see Fig. 1(a)). A body frame $\mathcal{C}_k = (k, \mathbf{x}_k, \mathbf{y}_k, \mathbf{z}_k)$ is fixed to particle k such that the unit vector $\mathbf{x}_k$ points in the direction of the velocity of particle k, $\mathbf{z}_k$ is the unit vector of the position $\mathbf{r}_k$, and $\mathbf{y}_k$ completes the right-handed reference frame.

A gyroscopic force steers each particle on the surface of the sphere. This force is modeled as a state-feedback control u_k that rotates the velocity of each particle about $\mathbf{z}_k$. The

(a) Frames $\mathcal{I}$ and $\mathcal{I}'$ (b) Frame $\mathcal{A}_k$

(c) Frame $\mathcal{B}_k$ (d) Frame $\mathcal{C}_k$ (e) Frame $\mathcal{D}_k$
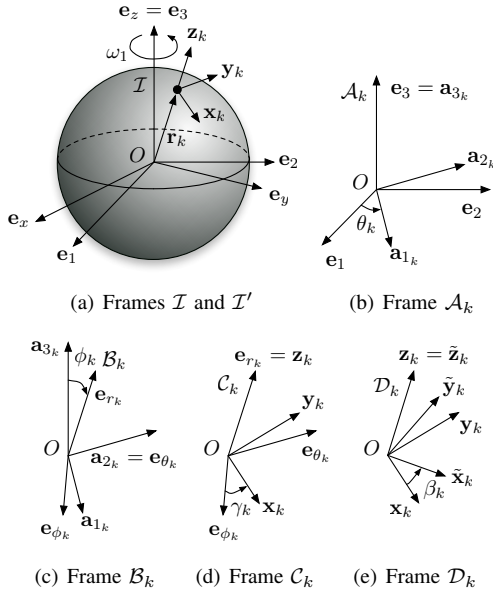
Fig. 1. Reference frames used to derive particle dynamics. Each frame differs from the previous one by a simple rotation. Note that frame $\mathcal{D}_k$ is not used until Section II-C.

equations of motion are [11]

$$
\begin{aligned}
\dot{\mathbf{r}}_k &= \rho_0 s_0 \mathbf{x}_k \\
\dot{\mathbf{x}}_k &= u_k \mathbf{y}_k - s_0 \mathbf{z}_k \\
\dot{\mathbf{y}}_k &= -u_k \mathbf{x}_k \\
\dot{\mathbf{z}}_k &= s_0 \mathbf{x}_k.
\end{aligned} \tag{1}
$$

Note that the dynamics in (1) represent a control system on the Lie group $SE(3)$ [5], [14].

B. Particle Dynamics on a Rotating Sphere

We extend the framework described in [11] by adding rotation to the sphere, which introduces a Coriolis effect. Coriolis acceleration contributes to the apparent deflection of each particle when viewed from a frame fixed to the sphere.

In order to derive the particle dynamics, we use a spherical coordinate system consisting of the azimuth angle θ_k, the polar angle ϕ_k and the (fixed) radius ρ_0. An inertial reference frame $\mathcal{I}$ is defined by $\mathcal{I} = (O, \mathbf{e}_x, \mathbf{e}_y, \mathbf{e}_z)$, where the origin O is located at the center of the sphere and $\mathbf{e}_x$, $\mathbf{e}_y$, and $\mathbf{e}_z$ are unit vectors (see Fig. 1). The sphere rotates at constant angular rate ω_1 about $\mathbf{e}_z$.

We introduce four additional reference frames. Frame $\mathcal{I}' = (O, \mathbf{e}_1, \mathbf{e}_2, \mathbf{e}_3)$ is fixed to the sphere and differs from $\mathcal{I}$ by a rotation of $\omega_1 t$ about $\mathbf{e}_3 = \mathbf{e}_z$, where t is time. Frame $\mathcal{A}_k = (O, \mathbf{a}_{1_k}, \mathbf{a}_{2_k}, \mathbf{a}_{3_k})$, $k \in \{1, \dots, N\}$, differs from $\mathcal{I}$ by a rotation of θ_k about $\mathbf{a}_{3_k} = \mathbf{e}_3$. Frame $\mathcal{B}_k = (O, \mathbf{e}_{\phi_k}, \mathbf{e}_{\theta_k}, \mathbf{e}_{r_k})$—the spherical body frame—differs from $\mathcal{A}_k$ by a rotation of ϕ_k about $\mathbf{e}_{\theta_k} = \mathbf{a}_{2_k}$. The unit vector $\mathbf{e}_{r_k}$ points from O to the position $\mathbf{r}_k$ of particle k. The fourth frame, $\mathcal{C}_k = (k, \mathbf{x}_k, \mathbf{y}_k, \mathbf{z}_k)$, differs from $\mathcal{B}_k$ by a rotation of the orientation angle γ_k about $\mathbf{z}_k = \mathbf{e}_{r_k}$. The origin of $\mathcal{C}_k$ is attached to particle k and the unit vector $\mathbf{x}_k$ points in the direction of motion of particle k relative to the sphere-fixed

frame $\mathcal{I}'$.[1]

The unit vectors of the four non-inertial reference frames are related by the following transformation table[2]

	$\mathbf{e}_1$	$\mathbf{e}_2$	$\mathbf{e}_3$	$\mathbf{e}_{\phi_k}$	$\mathbf{e}_{\theta_k}$	$\mathbf{e}_{r_k}$
$\mathbf{a}_{1_k}$	$\cos\theta_k$	$\sin\theta_k$	0	$\cos\phi_k$	0	$\sin\phi_k$
$\mathbf{a}_{2_k}$	$-\sin\theta_k$	$\cos\theta_k$	0	0	1	0
$\mathbf{a}_{3_k}$	0	0	1	$-\sin\phi_k$	0	$\cos\phi_k$
$\mathbf{x}_k$	$*$	$*$	$*$	$\cos\gamma_k$	$\sin\gamma_k$	0
$\mathbf{y}_k$	$*$	$*$	$*$	$-\sin\gamma_k$	$\cos\gamma_k$	0
$\mathbf{z}_k$	$*$	$*$	$*$	0	0	1

The angular velocity $^{\mathcal{I}}\boldsymbol{\omega}^{\mathcal{C}_k}$ of frame $\mathcal{C}_k$ with respect to the inertial frame $\mathcal{I}$ is $^{\mathcal{I}}\boldsymbol{\omega}^{\mathcal{C}_k} = (\omega_1 + \dot{\theta}_k)\mathbf{a}_{3_k} + \dot{\phi}_k \mathbf{e}_{\theta_k} + \dot{\gamma}\mathbf{z}_k$, where $\mathbf{a}_{3_k} = -\sin\phi_k \mathbf{e}_{\phi_k} + \cos\phi_k \mathbf{e}_{r_k} = -\sin\phi_k \cos\gamma_k \mathbf{x}_k + \sin\phi_k \sin\gamma_k \mathbf{y}_k + \cos\phi_k \mathbf{z}_k$ and $\mathbf{e}_{\theta_k} = \sin\gamma_k \mathbf{x}_k + \cos\gamma_k \mathbf{y}_k$ are found from the transformation table.

Taking the cross-product of the angular velocity $^{\mathcal{I}}\boldsymbol{\omega}^{\mathcal{C}_k}$ with a unit vector in frame $\mathcal{C}_k$ yields the inertial time-derivative of the unit vector, e.g., $\frac{^{\mathcal{I}}d}{dt}\mathbf{x}_k = {}^{\mathcal{I}}\boldsymbol{\omega}^{\mathcal{C}_k} \times \mathbf{x}_k$. We have

$$
\begin{aligned}
\frac{^{\mathcal{I}}d}{dt}\mathbf{x}_k &= (\cos\phi_k(\dot{\theta}_k + \omega_1) + \dot{\gamma}_k)\mathbf{y}_k \\
&\quad - (\sin\phi_k \sin\gamma_k(\dot{\theta}_k + \omega_1) + \cos\gamma_k \dot{\phi}_k)\mathbf{z}_k \quad (2)
\end{aligned}
$$

$$
\begin{aligned}
\frac{^{\mathcal{I}}d}{dt}\mathbf{y}_k &= -(\cos\phi_k(\dot{\theta}_k + \omega_1) + \dot{\gamma}_k)\mathbf{x}_k \\
&\quad - (\sin\phi_k \cos\gamma_k(\dot{\theta}_k + \omega_1) - \sin\gamma_k \dot{\phi}_k)\mathbf{z}_k \quad (3)
\end{aligned}
$$

$$
\begin{aligned}
\frac{^{\mathcal{I}}d}{dt}\mathbf{z}_k &= (\sin\phi_k \sin\gamma_k(\dot{\theta}_k + \omega_1) + \cos\gamma_k \dot{\phi}_k)\mathbf{x}_k \\
&\quad + (\sin\phi_k \cos\gamma_k(\dot{\theta}_k + \omega_1) - \sin\gamma_k \dot{\phi}_k)\mathbf{y}_k. \quad (4)
\end{aligned}
$$

The inertial kinematics of particle k expressed as vector components in frame $\mathcal{C}_k$ are computed as follows. The position of particle k with respect to O is $\mathbf{r}_k = \rho_0 \mathbf{z}_k$. The velocity is

$$
\begin{aligned}
\frac{^{\mathcal{I}}d}{dt}\mathbf{r}_k &= \rho_0 \Big[(\sin\phi_k \sin\gamma_k(\dot{\theta}_k + \omega_1) + \cos\gamma_k \dot{\phi}_k)\mathbf{x}_k \\
&\quad + (\sin\phi_k \cos\gamma_k(\dot{\theta}_k + \omega_1) - \sin\gamma_k \dot{\phi}_k)\mathbf{y}_k\Big]. \quad (5)
\end{aligned}
$$

The acceleration $\frac{^{\mathcal{I}}d^2}{dt^2}\mathbf{r}_k$ is found similarly.

The total force, $\mathbf{F}_k$, on particle k is the sum of the constraint (normal) force N_k that acts orthogonally to the surface of the sphere and the gyroscopic (steering) force u_k that acts tangentially to the surface of the sphere and orthogonally to $\mathbf{x}_k$, i.e., $\mathbf{F}_k = -N_k \rho_0 m_k \mathbf{z}_k + u_k \rho_0 m_k s_0 \mathbf{y}_k$, where m_k is the mass of particle k and $\rho_0 s_0$ is the (constant) speed of particle k. Note, we have scaled the force vector components by ρ_0 and m_k to eliminate these variables from the equations of motion.

Using Newton's second law, $\mathbf{F}_k = m_k \frac{^{\mathcal{I}}d^2}{dt^2}\mathbf{r}_k$, and $\frac{^{\mathcal{I}}d^2}{dt^2}\mathbf{r}_k$,

---

[1]We drop the subscript and use an arrow to denote the matrix collection of N elements, e.g., $\vec{\mathbf{r}} \triangleq [\mathbf{r}_1^T \cdots \mathbf{r}_N^T]^T$ and $\vec{\mathbf{x}} \triangleq [\mathbf{x}_1^T \cdots \mathbf{x}_N^T]^T$.

[2]Entries marked $*$ can be computed from the other entries.

we obtain

$$0 = 2\cos\phi_k\sin\gamma_k(\dot{\theta}_k + \omega_1)\dot{\phi}_k + \sin\phi_k\sin\gamma_k\ddot{\theta}_k$$
$$+ \cos\gamma_k\ddot{\phi}_k - \sin\phi_k\cos\phi_k\cos\gamma_k(\dot{\theta}_k + \omega_1)^2 \quad (6)$$
$$u_k s_0 = 2\cos\phi_k\cos\gamma_k(\dot{\theta}_k + \omega_1)\dot{\phi}_k + \sin\phi_k\cos\gamma_k\ddot{\theta}_k$$
$$- \sin\gamma_k\ddot{\phi}_k + \sin\phi_k\cos\phi_k\sin\gamma_k(\dot{\theta}_k + \omega_1)^2 \quad (7)$$
$$N_k = \sin^2\phi_k(\dot{\theta}_k + \omega_1)^2 + \dot{\phi}_k^2. \quad (8)$$

We solve (6) and (7) to obtain the equations of motion for θ_k and ϕ_k,

$$\ddot{\theta}_k = \frac{1}{\sin\phi_k}(u_k s_o \cos\gamma_k - 2\cos\phi_k(\dot{\theta}_k + \omega_1)\dot{\phi}_k)$$
$$\ddot{\phi}_k = -u_k s_0 \sin\gamma_k + \sin\phi_k\cos\phi_k(\dot{\theta}_k + \omega_1)^2. \quad (9)$$

We now derive the dynamics of particle k in the sphere-fixed frame, $\mathcal{I}'$. We have the kinematic relationship

$$\dot{\mathbf{r}}_k \triangleq \frac{\mathcal{I}'d}{dt}\mathbf{r}_k = \frac{\mathcal{I}d}{dt}\mathbf{r}_k\bigg|_{\omega_1=0}$$

By assumption, the movement of particle k relative to the sphere-fixed frame is parallel to $\mathbf{x}_k$, which implies $\dot{\mathbf{r}}_k \cdot \mathbf{y}_k = 0$. We also know that the particle speed relative to $\mathcal{I}'$ is $\rho_0 s_0$, i.e., $\|\dot{\mathbf{r}}_k\| = \rho_0 s_0$. Applying these two constraints to $\dot{\mathbf{r}}_k$ using (5) with $\omega_1 = 0$ yields

$$\sin\phi_k\cos\gamma_k\dot{\theta}_k - \sin\gamma_k\dot{\phi}_k = 0$$
$$\sin\phi_k\sin\gamma_k\dot{\theta}_k + \cos\gamma_k\dot{\phi}_k = s_0. \quad (10)$$

We solve (10) to obtain

$$\sin\gamma_k = \frac{\sin\phi_k\dot{\theta}_k}{s_0} \text{ and } \cos\gamma_k = \frac{\dot{\phi}_k}{s_0}. \quad (11)$$

We use the same procedure to find the dynamics of $\mathcal{C}_k$ in frame $\mathcal{I}'$. Applying (10) to (2)–(4) yields

$$\dot{\mathbf{x}}_k \triangleq \frac{\mathcal{I}'d}{dt}\mathbf{r}_k = \frac{\mathcal{I}d}{dt}\mathbf{r}_k\bigg|_{\omega_1=0} = \tilde{u}_k\mathbf{y}_k - s_0\mathbf{z}_k$$
$$\dot{\mathbf{y}}_k = \frac{\mathcal{I}'d}{dt}\mathbf{r}_k = \frac{\mathcal{I}d}{dt}\mathbf{r}_k\bigg|_{\omega_1=0} = -\tilde{u}_k\mathbf{x}_k \quad (12)$$
$$\dot{\mathbf{z}}_k = \frac{\mathcal{I}'d}{dt}\mathbf{r}_k = \frac{\mathcal{I}d}{dt}\mathbf{r}_k\bigg|_{\omega_1=0} = s_0\mathbf{x}_k,$$

where

$$\tilde{u}_k = \cos\phi_k\dot{\theta}_k + \dot{\gamma}_k.$$

Differentiating $\sin\gamma_k$ given in (11) with respect to time and using (9), we find

$$\tilde{u}_k = u_k - 2\omega_1\cos\phi_k.$$

Since $\cos\phi_k = \mathbf{z}_k \cdot \mathbf{e}_3 = z_{k_3}$ from the transformation table, we have

$$\tilde{u}_k = u_k - 2\omega_1 z_{k_3}. \quad (13)$$

Therefore, the dynamics of particle k relative to the sphere-fixed frame $\mathcal{I}'$ are

$$\dot{\mathbf{r}}_k = \rho_0 s_0\mathbf{x}_k$$
$$\dot{\mathbf{x}}_k = \tilde{u}_k\mathbf{y}_k - s_0\mathbf{z}_k$$
$$\dot{\mathbf{y}}_k = -\tilde{u}_k\mathbf{x}_k \quad (14)$$
$$\dot{\mathbf{z}}_k = s_0\mathbf{x}_k,$$

where $\tilde{u}_k$ is given by (13).

Note, since $\mathbf{r}_k = \rho_0\mathbf{z}_k$, the dynamics of particle k are fully described by either the set $\mathbf{r}_k$, $\mathbf{x}_k$, and $\mathbf{y}_k$ or the set $\mathbf{x}_k$, $\mathbf{y}_k$, and $\mathbf{z}_k$. The dynamics in (14) represent a control system on the Lie group $SE(3)$ [5], [14]. They can also be written as dynamics that evolve on $SO(3)$ according to

$$\dot{R}_k = R_k\hat{\boldsymbol{\xi}}_k = \begin{bmatrix} \mathbf{x}_k & \mathbf{y}_k & \mathbf{z}_k \end{bmatrix} \begin{bmatrix} 0 & -\tilde{u}_k & s_0 \\ \tilde{u}_k & 0 & 0 \\ -s_0 & 0 & 0 \end{bmatrix}, \quad (15)$$

where $\hat{\boldsymbol{\xi}}_k$ is an element of $so(3)$, the Lie algebra of $SO(3)$.

C. Particle Dynamics in a Time-Invariant Flowfield

We now study the case of N particles traveling on the surface of a rotating sphere in a time-invariant flowfield. The velocity of the flow at the position $\mathbf{r}_k$ is represented by $\mathbf{f}_k = \mathbf{f}(\mathbf{r}_k)$, which can be decomposed into vector components in frame $\mathcal{C}_k$:

$$\mathbf{f}(\mathbf{r}_k) = \rho_0(p_k\mathbf{x}_k + t_k\mathbf{y}_k), \quad (16)$$

where $p_k = \rho_0^{-1}(\mathbf{f}_k \cdot \mathbf{x}_k)$ and $t_k = \rho_0^{-1}(\mathbf{f}_k \cdot \mathbf{y}_k)$. (The dot product $\mathbf{f}_k \cdot \mathbf{z}_k$ is identically zero, due to the fact that $\mathbf{z}_k$ is perpendicular to the flow.) We assume that the flow is known and may be spatially non-uniform, as long as it is continuously differentiable. It must also satisfy $\|\mathbf{f}_k\| < \rho_0 s_0$, $\forall k$, to ensure that a particle can always make forward progress as measured from the rotating frame $\mathcal{I}'$. Adding (16) to the time derivative of the position of the particle model in (14) we obtain

$$\dot{\mathbf{r}}_k = \rho_0 s_0\mathbf{x}_k + \rho_0(p_k\mathbf{x}_k + t_k\mathbf{y}_k). \quad (17)$$

Knowing $\dot{\mathbf{r}}_k$, the rest of the components that fully describe the model can be found by computing the skew-symmetric matrix

$$\hat{\boldsymbol{\eta}}_k = \begin{bmatrix} 0 & -\tilde{u}_k & s_0 + p_k \\ \tilde{u}_k & 0 & t_k \\ -s_0 - p_k & -t_k & 0 \end{bmatrix}, \quad (18)$$

such that $\dot{R}_k = R_k\hat{\boldsymbol{\eta}}_k$, where $R_k \triangleq [\mathbf{x}_k \ \mathbf{y}_k \ \mathbf{z}_k] \in SO(3)$. The equations of motion are

$$\dot{\mathbf{r}}_k = \rho_0(s_0 + p_k)\mathbf{x}_k + \rho_0 t_k\mathbf{y}_k$$
$$\dot{\mathbf{x}}_k = \tilde{u}_k\mathbf{y}_k - (s_0 + p_k)\mathbf{z}_k$$
$$\dot{\mathbf{y}}_k = -\tilde{u}_k\mathbf{x}_k - t_k\mathbf{z}_k \quad (19)$$
$$\dot{\mathbf{z}}_k = (s_0 + p_k)\mathbf{x}_k + t_k\mathbf{y}_k,$$

where $p_k = \rho_0^{-1}(\mathbf{f}_k \cdot \mathbf{x}_k)$, $t_k = \rho_0^{-1}(\mathbf{f}_k \cdot \mathbf{y}_k)$ and $\tilde{u}_k = u_k - 2\omega_1 z_{k_3}$.

In order to find a control law to stabilize a formation in a time-invariant flow, we transform the dynamics of (19) using frame $\mathcal{D}_k = (k, \tilde{\mathbf{x}}_k, \tilde{\mathbf{y}}_k, \tilde{\mathbf{z}}_k)$, shown in Fig. 1(e). The motion of a particle in a flow can be determined by summing the motion of the particle relative to the flow and the motion of the flow relative to the sphere, such that $\tilde{\mathbf{x}}_k$ is parallel to $\frac{\mathcal{I}'d}{dt}\mathbf{r}_k$. The dynamics in frame $\mathcal{D}_k$ are

$$\dot{\tilde{\mathbf{r}}}_k = \rho_0 s_k\tilde{\mathbf{x}}_k$$
$$\dot{\tilde{\mathbf{x}}}_k = \nu_k\tilde{\mathbf{y}}_k - s_k\tilde{\mathbf{z}}_k$$
$$\dot{\tilde{\mathbf{y}}}_k = -\nu_k\tilde{\mathbf{x}}_k \quad (20)$$
$$\dot{\tilde{\mathbf{z}}}_k = s_k\tilde{\mathbf{x}}_k.$$

In (20), $\rho_0 s_k > 0$ is the (variable) speed of particle k relative to $\mathcal{I}'$ and ν_k is the control input. Since $\tilde{\mathbf{z}}_k = \mathbf{z}_k$ and $\tilde{\mathbf{r}}_k = \mathbf{r}_k$, we use (19) and (20) to write the following identity,

$$\tilde{\mathbf{x}}_k = s_k^{-1}\left[(s_0 + p_k)\,\mathbf{x}_k + t_k\mathbf{y}_k\right]. \qquad (21)$$

The reference frames $\mathcal{C}_k$ and $\mathcal{D}_k$ are related by the following transformation table:

	$\mathbf{x}_k$	$\mathbf{y}_k$	$\mathbf{z}_k$
$\tilde{\mathbf{x}}_k$	$s_k^{-1}(s_0 + p_k)$	$s_k^{-1}t_k$	0
$\tilde{\mathbf{y}}_k$	$-s_k^{-1}t_k$	$s_k^{-1}(s_0 + p_k)$	0
$\tilde{\mathbf{z}}_k$	0	0	1

(22)

From (21), the value of s_k is

$$s_k = \|s_k\tilde{\mathbf{x}}_k\| = \sqrt{(s_0 + p_k)^2 + t_k^2}. \qquad (23)$$

In practice, p_k and t_k are unknown. Therefore, in order to integrate (20) we must express s_k in terms of $\tilde{\mathbf{x}}_k$, $\tilde{\mathbf{y}}_k$, and $\mathbf{f}_k$ (expressed in the inertial frame). Such an expression for s_k is provided in the Appendix.

We find a relationship between ν_k and u_k by taking the time derivative on each side of (21) and comparing terms, to obtain

$$u_k = \nu_k + \left[\frac{s_k\dot{p}_k - \dot{s}_k(s_0 + p_k)}{s_k t_k}\right]. \qquad (24)$$

Since $s_k > 0$, (24) is non-singular even with $t_k = 0$. If $t_k = 0$, then $\mathbf{x}_k \cdot \tilde{\mathbf{x}}_k = 1$. Using (22), this implies

$$\begin{aligned} s_k &= s_0 + p_k \\ \dot{s}_k &= \dot{p}_k. \end{aligned} \qquad (25)$$

Substituting (25) into (24) yields

$$\lim_{t_k \to 0} u_k = \lim_{t_k \to 0}\left[\nu_k + \frac{\dot{s}_k - \dot{s}_k}{t_k}\right] = \nu_k. \qquad (26)$$

This can be used to prove that (24) is nonsingular and, as a result, it is possible to compute u_k from ν_k. Therefore, we use (20) and not (19) in the sequel.

III. Lyapunov-Based Control Design

We seek to design a decentralized control law that stabilizes circular motion with a common radius, axis of rotation and direction of rotation [11]. A circular trajectory on the surface of a sphere is the intersection of the sphere and a right circular cone whose axis of rotation passes through the center of the sphere and whose apex is outside the sphere. The position $\mathbf{c}_k$ (relative to the origin O) of the apex of the cone is [11]

$$\mathbf{c}_k = \mathbf{r}_k + \rho_0 s_0 \omega_0^{-1}\mathbf{y}_k, \qquad (27)$$

where $\omega_0 \neq 0$ and the chordal radius of the circle is $s_0\omega_0^{-1}$. The velocity of $\mathbf{c}_k$ along solutions of (14) with $\omega_1 = 0$ (i.e., on a non-rotating sphere), is $\dot{\mathbf{c}}_k \triangleq \frac{\mathcal{I}'d}{dt}\mathbf{c}_k = \rho_0 s_0(1 - \omega_0^{-1}u_k)\mathbf{x}_k$.

Proposition 1: [11, Proposition 2] For $\omega_1 = 0$, the (constant) control $u_k = \omega_0$ steers particle k around a circle such that the apex $\mathbf{c}_k$ of the associated cone is fixed, i.e., $\dot{\mathbf{c}}_k = \mathbf{0}$. A circular formation is characterized by the condition $\mathbf{c}_k = \mathbf{c}_j$ for all pairs j and k, where $\mathbf{c}_k$ is called the center of the circular formation.

A. Stabilization of a Circular Formation on a Rotating Sphere

Let $G = (\mathcal{N}, E)$ denote a time-invariant and undirected graph with graph Laplacian L [4]. The quadratic potential [11]

$$S(\vec{\mathbf{r}}, \vec{\mathbf{x}}, \vec{\mathbf{y}}, \vec{\mathbf{z}}) \triangleq \frac{1}{2}\vec{\mathbf{c}}^T \vec{L}\vec{\mathbf{c}} = \frac{1}{2}\sum_{(j,k)\in E}\|\mathbf{c}_j - \mathbf{c}_k\|^2, \qquad (28)$$

where $\vec{L} \triangleq L \otimes I_3$ and $\mathbf{c}_k$ is defined in (27), is minimized by the set of circular formations on a sphere. Let $\vec{L}_k$, $k \in \mathcal{N}$, denote three consecutive rows of $\vec{L}$ starting with row $3k-2$. The time derivative of S along solutions of (14) with $\omega_1 = 0$ is

$$\dot{S} = \sum_{j=1}^{N}\dot{\mathbf{c}}_j \cdot \vec{L}_j\vec{\mathbf{c}} = \sum_{j=1}^{N}\rho_0 s_0(1 - \omega_0^{-1}u_j)\mathbf{x}_j \cdot \vec{L}_j\vec{\mathbf{c}}. \qquad (29)$$

Choosing the control law

$$u_k = \omega_0(1 + K_0\rho_0 s_0\mathbf{x}_k \cdot \vec{L}_k\vec{\mathbf{c}}),\ K_0 > 0, \qquad (30)$$

ensures that S is nonincreasing [11].

Theorem 1: Let L be the Laplacian of a time-invariant, undirected and connected graph G. All solutions of the particle model (14) with $\omega_1 = 0$ (non-rotating sphere) and shape control (30) converge to the set of colocated circular trajectories on the same or opposite sides of the sphere with chordal radius $s_0\omega_0^{-1}$ and direction of rotation determined by the sign of ω_0. All solutions consisting of colocated circular trajectories on opposite sides of the sphere are unstable.

Proof: By the invariance principle, all solutions converge to the largest invariant set where $\mathbf{x}_k \cdot (\mathbf{c}_k - \mathbf{c}_j) = 0$ for all connected pairs j and k. This is a set of circular trajectories on the same or opposite sides of the sphere. Suppose M particles are on one side of the sphere and $N-M$ particles are on the other side. By considering the change in S as a function of a variation of a particle in either group, we observe that (1) if N is even, then solutions with $M = N/2$ are local maxima; and (2) for any $N > 2$, solutions with $N > M > 0$ are saddles. Therefore, all solutions consisting of colocated circular trajectories on opposite sides of the sphere are unstable. ∎

We now consider particle model (14) with $\omega_1 \neq 0$. Using the control law (30) stabilizes a circular formation on the rotating sphere, but the center is not fixed (see Fig. 2 (a)). We stabilize a circular formation with a fixed center by choosing

$$\begin{aligned} \tilde{u}_k &= u_k - 2\omega_1 z_{k_3} \\ &= \omega_0(1 + K_0\rho_0 s_0\mathbf{x}_k \cdot \vec{L}_k\vec{\mathbf{c}}) - 2\omega_1 z_{k_3}, \end{aligned} \qquad (31)$$

where $K_0 > 0$. The control (31) cancels the Coriolis effect (see Fig. 2 (b)).

Corollary 1: For the rotating model (14) with $\omega_1 \neq 0$, choosing the control (31) cancels the Coriolis effect from the dynamics and stabilizes the set of circular formation whose center is fixed relative to the sphere and has chordal radius $s_0\omega_0^{-1}$ and direction of motion determined by the sign of ω_0.

(a)   (b)
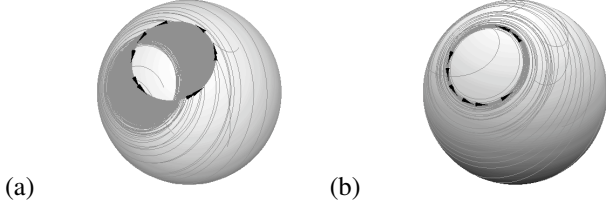
Fig. 2. Stabilization of a circular formation on a rotating sphere using (14) with a Laplacian control. Parameter values used in both simulations are $N = 10$, $s_0 = 1$, $\rho_0 = 10$, $\omega_0 = 2$, $\omega_1 = 0.1$ and $K_0 = 0.01$. (a) Control (30) stabilizes a circular formation on a rotating sphere, but the formation is translated along the sphere due to the Coriolis effect. (b) Control (31) cancels the Coriolis effect and stabilizes a circular formation with a fixed center.

B. Stabilization of a Circular Formation in a Time-Invariant Flowfield

We now work in the frame $\mathcal{D}_k$ and find a control law that stabilizes a circular formation in a time-invariant flow on a rotating sphere. In $\mathcal{D}_k$, the center of the circular formation is

$$\tilde{\mathbf{c}}_k = \tilde{\mathbf{r}}_k + \rho_0 s_0 \omega_0^{-1} \tilde{\mathbf{y}}_k. \tag{32}$$

The velocity of $\tilde{\mathbf{c}}_k$ along solutions of (20) is $\dot{\tilde{\mathbf{c}}}_k \triangleq \frac{\mathcal{I}' d}{dt} \tilde{\mathbf{c}}_k = \rho_0 (s_k - s_0 \omega_0^{-1} \nu_k) \tilde{\mathbf{x}}_k$.

Lemma 1: The control $\nu_k = \omega_0 s_0^{-1} s_k$ steers particle k around a circle such that the apex $\tilde{\mathbf{c}}_k$ of the associated cone is fixed.

Proof: Substituting $\nu_k = \omega_0 s_0^{-1} s_k$ into $\dot{\tilde{\mathbf{c}}}_k$ yields $\dot{\tilde{\mathbf{c}}}_k = \rho_0 (s_k - s_0 \omega_0^{-1} \nu_k) \tilde{\mathbf{x}}_k = \rho_0 (s_k - s_k) \tilde{\mathbf{x}}_k = \mathbf{0}$. ∎

Again, let $G = (\mathcal{N}, E)$ denote a time-invariant and undirected graph with graph Laplacian L. The quadratic potential

$$S(\vec{\tilde{\mathbf{r}}}, \vec{\tilde{\mathbf{x}}}, \vec{\tilde{\mathbf{y}}}, \vec{\tilde{\mathbf{z}}}) \triangleq \frac{1}{2} \vec{\tilde{\mathbf{c}}}^T \vec{L} \vec{\tilde{\mathbf{c}}} = \frac{1}{2} \sum_{(j,k) \in E} \| \tilde{\mathbf{c}}_j - \tilde{\mathbf{c}}_k \|^2, \tag{33}$$

where $\vec{L} \triangleq L \otimes I_3$ and $\tilde{\mathbf{c}}_k$ is defined in (32), is minimized by the set of circular formations on the sphere. The time derivative of S along solutions of (20) is

$$\dot{S} = \sum_{j=1}^{N} \dot{\tilde{\mathbf{c}}}_j \cdot \vec{L}_j \vec{\tilde{\mathbf{c}}} = \sum_{j=1}^{N} \rho_0 (s_k - \frac{s_0}{\omega_0} \nu_j) \tilde{\mathbf{x}}_j \cdot \vec{L}_j \vec{\tilde{\mathbf{c}}}. \tag{34}$$

Choosing the control law

$$\nu_k = \frac{\omega_0}{s_0} (s_k + K_1 \tilde{\mathbf{x}}_k \cdot \vec{L}_k \vec{\tilde{\mathbf{c}}}), \ K_0 > 0, \tag{35}$$

ensures that S is nonincreasing.

Theorem 2: Let L be the Laplacian of a time-invariant, undirected and connected graph G. Let $\mathbf{f}_k = \mathbf{f}(\mathbf{r}_k)$ be a time-invariant flow satisfying $\|\mathbf{f}\| < \rho_0 s_0$. All solutions of the particle model (20) with shape control (35) converge to the set of colocated circular trajectories on the same or opposite sides of the sphere with chordal radius $s_0 \omega_0^{-1}$ and direction of rotation determined by the sign of ω_0. All solutions consisting of colocated circular trajectories on opposite sides of the sphere are unstable.

(a)   (b)
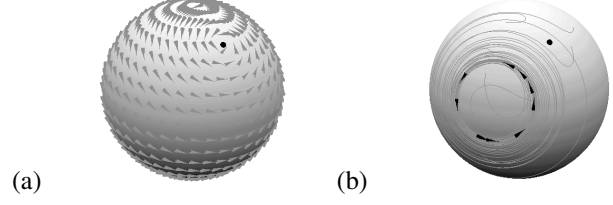
Fig. 3. Stabilization of a circular formation in a point-vortex generated flow. The vortex is represented by the black dot, with $\Gamma = 1$. (a) The flowfield rotates around the vortex. (b) Control (35) stabilizes a circular formation near a point vortex. Parameter values used are $N = 10$, $s_0 = 1$, $\rho_0 = 3$, $\omega_0 = 2$, $K_0 = 0.1$ and $\omega_1 = 0.05$.

IV. EXAMPLE: POINT-VORTEX GENERATED FLOW

A vortex is a spinning flowfield. The vortex strength is given by Γ, the circulation [9]. Given a flowfield $\mathbf{f}(\mathbf{r}_k)$, the associated vorticity field $\boldsymbol{\Omega}_k$ is the curl of the flowfield,

$$\boldsymbol{\Omega}_k = \nabla \times \mathbf{f}(\mathbf{r}_k).$$

The flow due to M point vortices on the surface of a sphere is [9]:

$$\mathbf{f}_i = \frac{1}{4\pi\rho_0} \sum_{j=1; j \neq i}^{M} \Gamma_j \frac{\mathbf{r}_j \times \mathbf{r}_i}{\rho_0^2 - \mathbf{r}_i \cdot \mathbf{r}_j}, \tag{36}$$

where ρ_0 is the radius of the sphere and $\mathbf{r}_j$ is the position of a vortex relative to the center of the sphere. In this paper we study point vortices in the context of model (20): first using one vortex to generate a time-invariant flow and then using two vortices to generate a time-varying flow.

A. Time-Invariant Flow: One Vortex on a Sphere

We study the case of a single point vortex generating a time-invariant flow in model (20). The control law used to stabilize a circular formation is defined in (35). Fig. 3 shows the results of a numerical simulation. Note, although the vortex singularity in (36) breaks the assumptions on the magnitude of the flow in Theorem 2, the formation is stabilized in simulation.

B. Time-Varying Flow: Two Vortices on a Sphere

The presence of a second vortex causes both vortices to move. We make the assumptions that the vortices affect the motion of the particles, but the particles do not affect the motion of the vortices. We also assume that the vortex motion does not experience the Coriolis effect. $3M$ equation are needed to solve the two-vortex problem on a sphere [9]. However, the constraint that the vortices lie on the surface of the sphere reduces the system to $2M$ equations. The Hamiltonian of the system (36) for $M = 2$ is [9]

$$H = \frac{\Gamma_1 \Gamma_2}{4\pi\rho_0} \log(l_{12}^2) = constant, \tag{37}$$

where l_{12} is the chordal distance between the two vortices. From H we can conclude that the distance between two

(a)   (b)
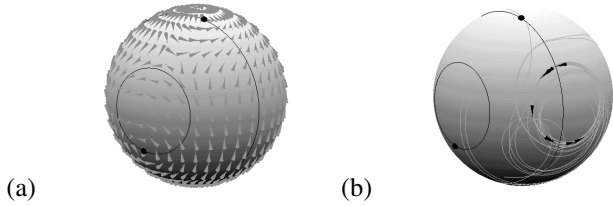
Fig. 4.   Stabilization of a circular formation with two vortices generating a time-varying flow. The two vortices are represented by black dots and $\Gamma_1 = 4$ and $\Gamma_2 = 2$. (a) Flowfield direction around vortices. Note how the flow spins around each vortex. (b) Control (35) stabilizes the particles into a circular formation near two vortices. Parameter values used are $N = 10$, $s_0 = 1$, $\rho_0 = 3$, $\omega_0 = 2$, $K_0 = 0.1$ and $\omega_1 = 0.05$. As a vortex passes through the circular formation, the particle motion changes direction, but the circular formation is maintained. Once the vortex has passed completely through the circular formation, the particle motion returns to its original direction.

vortices remains fixed, so that all solutions form relative equilibria. Also, the center of vorticity,

$$\mathbf{C} = \frac{\Gamma_1 \mathbf{r}_1 + \Gamma_2 \mathbf{r}_2}{\Gamma_1 + \Gamma_2} = constant, \qquad (38)$$

is an invariant of the system.

Equations (37) and (38) give rise to the four equations necessary to solve the problem. In general, two vortices will each move on the base of a fixed cone whose plane is perpendicular to $\mathbf{C}$. The vortex with a larger Γ will move on the base of the cone of smaller radius. If $\Gamma_1 = \Gamma_2$, the vortices will move on the same plane perpendicular to $\mathbf{C}$ on opposite sides of the same cone. Fig. 4 shows a simulated example, which suggests that the time-invariant control may apply to certain time-varying flowfields.

V. Conclusion

The models studied here are of particular interest because they can be used to study realistic occurrences on the Earth. For example, the rotating sphere model depicts the Earth spinning on its axis, while vortices are used to depict ocean currents, hurricanes and tornadoes. The purpose of this research is to stabilize collective motion of autonomous vehicles in air and sea that are subject to these phenomena. In this paper we have provided theoretically justified algorithms that stabilize circular formations on the surface of a rotating sphere in a time-invariant flow. Simulations suggest that these algorithms are applicable to flows that exceed the particle speed and to time-varying flows. In ongoing work, we seek to provide theoretical justification of these observations. In addition, we plan to validate the performance of these control algorithms in real flow data.

References

[1] R. W. Beard, T. W. McLain, D. B. Nelson, D. Kingston, and D. Johanson. Decentralized cooperative aerial surveillance using fixed-wing miniature UAVs. *Proc. IEEE*, 94(7):1306–1324, 2006.

[2] R. E. Davis, C. E. Eriksen, and C. P. Jones. Autonomous buoyancy-driven underwater gliders. In G. Griffiths, editor, *The Technology and Applications of Autonomous Underwater Vehicles*, chapter 3, pages 37–58. Taylor and Francis, 2002.

[3] J. Elston and E. Frew. Unmanned aircraft guidance for penetration of pre-tornadic storms. In *Proc. AIAA Guidance, Navigation and Control Conf. and Exhibit (electronic)*, number AIAA-2008-6513, Honolulu, Hawaii, 2008. (16 pages).

[4] C. Godsil and G. Royle. *Algebraic Graph Theory*. Number 207 in Graduate Texts in Mathematics. Springer-Verlag, 2001.

[5] E. W. Justh and P. S. Krishnaprasad. Natural frames and interacting particles in three dimensions. In *Proc. Joint 44th IEEE Conf. Decision and Control and European Control Conf.*, pages 2841–2846, Seville, Spain, December 2005.

[6] D. B. Kingston. *Decentralized Control of Multiple UAVs for Perimeter and Target Surveillance*. PhD thesis, Department of Electrical and Computer Engineering, Brigham Young University, Provo, Utah, December 2007.

[7] D. J. Klein and K. A. Morgansen. Controlled collective motion for trajectory tracking. In *Proc. 2006 American Control Conf.*, pages 5269–5275, Minneapolis, Minnesota, June 2006.

[8] N. E. Leonard, D. A. Paley, F. Lekien, R. Sepulchre, D. M. Fratantoni, and R. E. Davis. Collective motion, sensor networks and ocean sampling. *Proc. IEEE*, 95(1):48–74, 2007.

[9] P. Newton. *The N-Vortex Problem*. Springer-Verlag, 2001.

[10] D. A. Paley. Cooperative control of an autonomous sampling network in an external flow field. In *Proc. 47th IEEE Conf. Decision and Control*, pages 3095-3100, Cancun, Mexico, December 2008.

[11] D. A. Paley. Stabilization of collective motion on a sphere. *Automatica*, 45(1):212–216, 2009.

[12] D. A. Paley and C. Peterson. Stabilization of collective motion in a time-invariant flow field. To appear in AIAA J. Guidance, Control, and Dynamics.

[13] L. Scardovi, N. E. Leonard, and R. Sepulchre. Stabilization of collective motion in three dimensions: A consensus approach. In *Proc. 46th IEEE Conf. Decision and Control*, pages 2931–2936, New Orleans, Louisiana, December 2007.

[14] L. Scardovi, R. Sepulchre, and N. E. Leonard. Stabilization laws for collective motion in three dimensions. pages 4591–4597, July 2007. In *Proc. European Control Conference*, Kos, Greece.

Appendix

In order to find the speed s_k from the dynamics (20), we perform the following calculations. From (16) and (23) we know:

$$s_k = \sqrt{(s_0 + p_k)^2 + t_k^2} \qquad (39)$$

$$p_k = \rho_0^{-1}(\mathbf{f}_k \cdot \mathbf{x}_k) \qquad (40)$$

$$t_k = \rho_0^{-1}(\mathbf{f}_k \cdot \mathbf{y}_k). \qquad (41)$$

Using (22), (40), and (41) we have

$$p_k = \frac{s_0 + p_k}{s_k}(\mathbf{f}_k \cdot \tilde{\mathbf{x}}_k) - \frac{t_k}{s_k}(\mathbf{f}_k \cdot \tilde{\mathbf{y}}_k) \qquad (42)$$

$$t_k = \frac{t_k}{s_k}(\mathbf{f}_k \cdot \tilde{\mathbf{x}}_k) + \frac{s_0 + p_k}{s_k}(\mathbf{f}_k \cdot \tilde{\mathbf{y}}_k). \qquad (43)$$

Equations (39), (42), and (43) form an algebraic system of three equations with three unknowns, where the unknowns are s_k, p_k, and t_k. This system of equations can be solved to find a polynomial $p(s_k)$:

$$\begin{aligned} p(s_k) &= \left[(s_k - a)^2 - \left(s_0^2 + b^2\right)\right]\left[(s_k - a)^2 + b^2\right] \\ &\quad + 2s_0 b^2 \sqrt{(s_k - a)^2 + b^2} = 0, \end{aligned}$$
$$(44)$$

where $a = (\mathbf{f}_k \cdot \tilde{\mathbf{x}}_k)$ and $b = (\mathbf{f}_k \cdot \tilde{\mathbf{y}}_k)$. Solving for s_k yields only one solution that satisfies the necessary condition $s_k > 0$.